

E-ISSN: 0976-4844 • Website: www.ijaidr.com • Email: editor@ijaidr.com

# Coordinated Control of FACTS Devices for Damping Power Oscillations

Mr. Chandan Kumar Sah<sup>1</sup>, Dr. A. S. Kannan<sup>2</sup>

<sup>1</sup>Research Scholar, <sup>2</sup>Associate Professor Department of Electrical Engineering Annamalai University.

### **Abstract:**

Maintaining power system stability has become increasingly challenging due to low-frequency oscillations arising from high renewable energy penetration, fluctuating loads, and inter-area interactions. Typically, these local Power Oscillation Damping (POD) controllers and decentralized FACTS-based methods that are used for damping may be slow in their reaction, have a limited degree of adaptability, and cannot effectively suppress inter-area oscillations, thus resulting in voltage, frequency, and rotor angle deviations. In order to get beyond these restrictions, this research introduces the Hierarchical Coordinated FACTS Damping Control Architecture (HCFDCA) using Hierarchical Graph Neural Network-assisted Multi-Agent Reinforcement Learning with Safety-Layered MPC (HGNN-MARL-MPC). The system merges the local POD controllers for SVC, STATCOM, TCSC, and UPFC devices with a supervisory coordination layer which by means of optimization controls the damping actions throughout the network. This approach is aimed at ensuring that oscillations are quickly brought under control, that the rotor angle and frequency deviations are kept to a minimum, that the voltage support is strengthened, and that the power flow stability is improved. The IEEE 39-bus and 118-bus test systems were used for the simulation experiments to check the effectiveness of the proposed model which, as a result, can reduce the peak rotor angle deviations by ~25%, increase the damping ratios from 0.09 to 0.23, and keep the maximum frequency deviations at 0.11 Hz. The stability margins under the 80-120% load variations have been raised from 45-60% to 80-90%, thus the method's robustness, scalability, and readiness for the integration into modern smart grids with wide-area measurements are emphasized.

**Keywords:** Flexible AC transmission devices, power oscillation damping, hierarchical coordinated control, damping enhancement, inter-area oscillations, power system stability, renewable energy integration.

### 1. Introduction

Stability and reliability during dynamic operating conditions is one of the greatest challenges in modern power system [1]. Grids of large scale connected with each other are usually prone to disruptions including load circling, line trips, or malfunctions at generators, and can cause low-frequency oscillations of power [2]. Unless dampened, such oscillations can cause a deterioration in the performance of the system or result in instability. Hence suitable damping of these vibrations is of paramount importance that guarantees safe and stable functioning of the electrical system, particularly with the growing complexity of the system and its level of interconnections [3]. FACTS devices have also become a potent instrument that can be used to improve the controllability and stability of power systems. FACTS devices enhance the capability of transfer of power, regulation of voltages and damping, by the dynamic adjustment of voltage, impedance and phase angle [4]. Examples of default FACTS controllers include Static Var Compensator (SVC), Thyristor-Controlled Series Capacitor



E-ISSN: 0976-4844 • Website: www.ijaidr.com • Email: editor@ijaidr.com

(TCSC) and Unified Power Flow Controller (UPFC) can adjust system parameters in real time, and therefore help to damp oscillations [5]. The autonomous functioning of these devices however does not normally perform optimally in large interconnected grids.

In order to overcome this drawback, coordinated controllers of FACTS devices have been proposed to improve the overall damping behavior with concerted and harmonized behaviors [6]. In coordinated control, a group of FACTS devices is used to provide effective damping of various modes of oscillations and to achieve this, the group of FACTS devices are used together under common control signals or optimized control laws. This kind of coordination assists in eliminating control conflicts, minimizing redundancy in actions and making sure that damping torques contributions of each device are globally optimized [7]. More recent studies have been devoted to improved methods of control such as adaptive control, model predictive control (MPC), and artificial intelligence (AI)-based coordination to enhance the dynamic response of FACTS devices when operating in different system conditions [8]. The methods allow achieving convergence in a shorter period of time, improved robustness, and real-time adjustability to disruptions [9]. The coordinated operation of FACTS devices is a central factor in the realization of resilient, stable, and efficient operation of a power system as the power grid is further developed to be more flexible and connected with renewable sources [10]. System stability issues that were easier to handle before are now more difficult to manage due to the increased use of renewable energy sources that are less predictable and the complexity of power grids that become more and more complicated [11]. Low-frequency oscillations of the power system that are usually within the range of 0.2–2.5 Hz tend to be strongly influenced by the renewables' fluctuating nature, load changes, and interarea interactions of large interconnected networks [12].

When the oscillations reach this level, the consequences might be very disruptive, ranging from an excessive increase in rotor angle swings to voltage instability, frequency deviations, and ultimately a blackout of a large part of a network. Local Power Oscillation Damping (POD) controllers or decentralized FACTS-based control methods acting individually have only a limited potential to solve the problem since they are characterized by a slow response, lack of adaptability to real-time changes, and usually in effectiveness of inter-area oscillations failure. The development of wide-area monitoring systems, advanced communication infrastructure, and intelligent control algorithms makes it possible to meet the latent need for a geographically coordinated, adaptive control strategy able to optimize the damping actions of multiple FACTS devices. This paper presents a hierarchical coordinated control framework using graph neural networks, multi-agent reinforcement learning, and safety-layered model predictive control as a response to the issues raised to improve system damping, reduce rotor angle and frequency deviations, and enhance voltage and power stability. This approach provides a scalable, robust, and forward-looking solution suitable for next-generation smart grids.

#### 2. Literature review

Some of the recent literatures related to this study has been discussed below,

Nahak & Satapathy, (2025) suggested Microgrid Low-Frequency Oscillation and GOV-PSS Coordination. Renewable-integrated microgrids exhibit high multiplied low-frequency oscillations in a disturbance of uncertainty. The suggested GOV-PSS controller coordinates the turbine governor and PSS, which improves the small-scale stability. The controller gains are optimized by a hybrid DE gray wolf approach. Critical oscillations occur due to random changes in PV, wind and reference voltages and these oscillations are effectively dampened by the controller. Tuning of the excitation without changing the voltage control. On a 9 and 33-bus-simulation, lower oscillations and a better rotor angle stability were observed, which validates feasibility of practical implementation.

Feng et al. 2025 deliberated the Suppression of broadband oscillations in wind dominated systems. The penetration of new energy sources is high which causes broadband oscillations. Further wind turbine damping and flexible DC interconnects controllers are developed. I-PGSA mode-tracking is used to optimize controller parameters to eliminate target offset. The results of eigenvalue analysis and



E-ISSN: 0976-4844 • Website: www.ijaidr.com • Email: editor@ijaidr.com

PSCAD/EMTDC simulation prove the suppression of broadband oscillations. The methodology provides sufficiently strong damping and rapid computing power. The oscillations are effectively mitigated and grid safety is improved.

Feng et al. 2025 discussed the Coordinated Damping and Inertia Control DERs. DEERs with converter interfaces are poorly damped and low inertia. Multi-DERs are co-ordinated through a hybrid system of damping and inertia allocation strategy that is applied to economic incentives. The optimization problem has the minima as the cost, frequency and small-signal stability. Convex parametric formulation can do away with tuning. The solution takes network coupling into account and promotes the collaboration of DER. It has been simulated that multi-DER integration will be more cost-effective and stable.

Ghatuari & Kumar, (2025) suggested EV-Based Frequency Co-ordination Regulating. Aggregated EVs also are used to provide rapid frequency control in grids across areas. PSO and CSA are used in optimization of controller parameters. The frequency deviations seen using the CSA-optimized controller are within the range of  $\pm 0.2$ Hz and the settling time is at 10s. Among the n-2 contingency tests, there is better ITAE. The outcome of the simulation on IEEE 9-bus signals stability improvement. The paper points at the grid frequency support of EVs.

Kumar & Koshta, (2025) deliberated Distributed Power Flow Controller (DPFC) of Line Control. The power-electronics-based controllers are replacing mechanical control of PFCDs. DPFC enables less costly and better reliability control on the level of UPFC. It eliminates the DC link giving the converters an opportunity to work independently. D-FACTS concepts are applied in series converters to reduce their costs. Pressure power is exchanged at the third harmonic frequency. DPFC provides an improved level of controllability and stability of power flow within the current grids.

Bernal-Sancho, et al. 2025 suggested a study on FFT-Based POD in Renewable penetrated grids. PV and wind combination leads to decreased inertia and augmented cross-area vibrations. FFT-based POD identifies and counters vibrations through dynamism. Optimization of controller parameters is done using Nobel Bat Algorithm. IEEE-39 simulations indicate that there is a high level of oscillation suppression and restoration of stability. When stability is attained POD automatically deactivates. The approach has regulatory compliance of wide-area oscillation damping.

Mateu-Barriendos et al. 2025 suggested POD Controllers of Reactors on Other Forms. The GFOR converters have POD controllers that are designed to damp electromechanical oscillations. With frequency-based inputs, active and passive as well as reactive power modulation (POD-P, POD-Q, POD-PQ) is employed. It works with small-scale stability and nonlinear simulation. The strategy is minimum measurements and is easy to apply. The eigenvalue-sensitivity designs are optimum controller designs. Findings: It shows enhanced damping in convertor-controlled systems.

Satapathy et al. 2025 deliberated the Hydro Governors Interacted with STATCOM. Negative damping is normally contributed by the hydro governors. Statcom Phase-compensated Hydro managers are coordinated, and enhance damping torque. Multi-objective MeDETVAPSO controller parameters are optimized with regard to performance. Multi-area and large IEEE simulations demonstrate shortened settling time, peak of oscillation, and large damping ratio. oniflog OPAL-RT results can be checked with real time simulation. The suggested approach is superior to traditional PSS, PSO and DE-tuned controllers. Following table 1 shows the research gap among the existing studies.

Table 1: Research gap

Author(s), Year	Proposed Technique	Significance / Key Findings	Limitations
	GOV-PSS controller	1	Limited to small MG setups;
Satapathy, 2025	with hybrid DE-gray wolf optimizer	oscillations in microgrids; improves rotor angle stability;	performance under large-scale



E-ISSN: 0976-4844 • Website: <a href="www.ijaidr.com">www.ijaidr.com</a> • Email: editor@ijaidr.com

		feasible on 9 & 33-bus systems	
Feng et al., 2025	Damping controllers with I-PGSA mode- tracking	Suppresses broadband oscillations in wind-dominated systems; fast computation; eigenvalue and PSCAD/EMTDC validated	Focused on wind-integrated systems; less on other DER types
Feng et al., 2025	Hybrid damping & inertia allocation for multiple DERs	Enhances frequency stability; cost-effective; network-wide coordination; convex formulation avoids iterative tuning	Economic incentives need practical validation; assumes cooperation among DERs
Ghatuari & Kumar, 2025	EV-based coordinated frequency control (PSO & CSA optimization)	Rapid frequency regulation; ±0.2 Hz deviation; 10 s settling; effective under N-2 contingencies	Dependent on EV availability; only IEEE 9-bus tested
Kumar & Koshta, 2025	Distributed Power Flow Controller (DPFC)	Reduces cost; improves reliability and stability; independent converter operation; D-FACTS concept	Requires specialized converters; third harmonic injection may need filtering
Bernal-Sancho et al., 2025	FFT-based POD with Nobel Bat Algorithm	Detects & mitigates inter-area oscillations dynamically; automatic deactivation; regulatory compliant	Limited to PV/wind systems; scalability for large grids not tested
Mateu- Barriendos et al., 2025	POD controllers for GFOR converters (POD-P, POD-Q, POD-PQ)	Damps electromechanical oscillations with minimal measurements; small-signal & nonlinear validated	Limited to converter- dominated systems; larger network effects not assessed
Satapathy et al., 2025	Hydro governor + STATCOM coordination with MeDETVAPSO	Shortens settling time; reduces oscillation peaks; increases damping ratio; validated in OPAL-RT	Focused on hydro-based systems; may not generalize to other synchronous generators

### 2.1 Problem statement

The concept of ensuring that power systems remain stable has grown to be more problematic with the large-scale penetration of renewable energy, variable loads, as well as affected interactions between areas. A high penetration of photovoltaic (PV) and wind generation would lower the inertia of a system, resulting in the grid being more vulnerable to the low frequency electromechanical oscillations that may adversely affect the rotor angle stability, frequency regulation and voltages. The conventional damping methods, like local Power Oscillation Damping (POD) controllers and decentralized FACTS based controllers, are slow to respond, lacks flexibility in its controls and does not have the capacity to detect inter-area vibrations, especially in a multi-area and in areas which contain renewable sources. Also, traditional means can be based on manually adjusted gains and do not provide real-time coordination, resulting in a poor performance under different load conditions, change of grid topology, and distortions. Recent pushed-networks Microgrids and distributed energy resource (DER) are no exceptions to this phenomenon, with weak damping, low inertia, and stochastic renewable injections contributing to oscillatory instabilities. Furthermore, new technologies such as electric vehicles (EVs) or grid-forming converters demand co-ordinated approaches to frequency support, but no known technology considers the optimisation of the network or cost concerns on a network-wide basis. These constraints bring an urgent requirement of a strong scalable and adaptive control architecture that can dynamically reduce



E-ISSN: 0976-4844 • Website: <a href="www.ijaidr.com">www.ijaidr.com</a> • Email: editor@ijaidr.com

oscillations, increase damping ratios, and make the system overall resilient. The issue is also increased due to the increasing complexity of today power systems which requires integrated multi-agent control principles capable of using wide-area measurements, predictive control and reinforcement learning to effectively suppress oscillations whilst still maintaining voltage stability, tie-line power regulation, and operational constraints.

## 3. Proposed model

The proposed system model of the coordinated FACTS-based damping is the model that enhances the integration of the physical power system and the cyber-control layers through a coherent framework. The prime mover torques or renewable energy injection are the mechanical inputs which are used to accelerate the synchronous generators which are modeled by classical swing equations coupled with the dynamics of an excitation system. Such equations represent the responses of the rotor angle  $(\delta)$  and speed  $(\omega)$  and are the fundamental electromechanical states which cause low-frequency oscillations. The transmission network links the generators in the form of algebraic power-flow equations. Such equations are used to relate bus voltages, currents and power flows (P,Q) in the network and implement the laws of Kirchhoff. FACTS devices, SVC, STATacom, TCSC and UPFC are represented as low-order dynamic systems, and the controllable states include shunt susceptance, series reactance or injected series voltage.

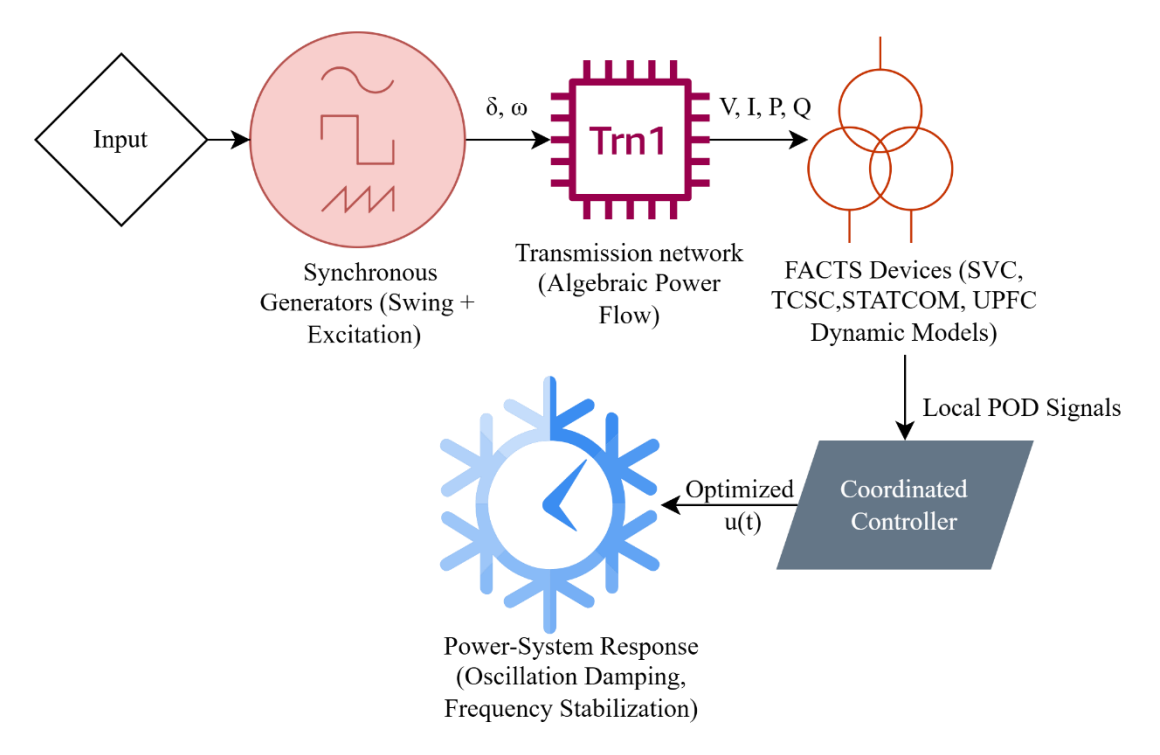


Figure 1: HGNN-MARL Coordinated FACTS Architecture

Devices have a local Power Oscillation Damping (POD) loop which produces additional control signals, depending on measurements of voltage deviations or power flow on location. The signals are fed into the device control input to enhance the damping of the electromechanical modes. By ensuring coordinated damping, all the FACTS devices are linked to a greater level controller through a hierarchical GNN-assisted multi-agent reinforcement learning structure that is integrated with an overlay of safety-based Model Predictive Control (HGNN-MARL-MPC). This layer takes inputs of local measurements, network-wide embeddings, and device states and computes optimized control inputs (t) which reduce both local and inter-area oscillations and comply with operational restrictions. This system is a modeled as a complex of differential-algebraic equations and can be linearized to perform small-signal stability



E-ISSN: 0976-4844 • Website: <a href="www.ijaidr.com">www.ijaidr.com</a> • Email: editor@ijaidr.com

analysis. The resulting state matrix is analysed using eigenvalue and participation factor analysis to identify poorly damped modes on which tuning of the controllers and placement of FACTS is based. The integrated modeling technique is used to guarantee that the physical and cyber-control dynamics are represented, such that the oscillation damping can be strong and coordinated with respect to the load and fault conditions. Figure 1 shows the HGNN-MARL Coordinated FACTS Architecture.

This research mainly depends on input data that reflects real-time power system conditions and is procured directly from phasor measurement units (PMUs) and a wide-area monitoring system (WAMS). Among these data are voltage magnitudes, phase angles, active power and reactive power flows, generator rotor speeds, and system frequency deviations. Besides system topology data, transmission line parameters, and generator control settings are introduced to dynamically model the interactions of the network components. The plant input data is used to implement oscillation detection, modal analysis, and the coordinated control of FACTS devices such as SSSC, STATCOM, and UPFC, leading to the correct localization and neutralization of low-frequency oscillations.

The work of this investigation is a coordinated control framework that, as a result, successfully elevates the power system's stability level through the damping of low-frequency power oscillations. In particular, it commands FACTS devices such as STATCOM, SSSC, and UPFC with optimized control signals, thus, their dynamic responses are concerted for damping oscillations efficiently. The framework brings about tangible effects on the system performance indicators, for example, the damping ratios become higher, the settling time is shorter, bus voltages become stable, and inter-area power swings are reduced. Furthermore, the simulation findings offer a quantitative confirmation via the shifts of eigenvalues, time-domain responses, and frequency-domain analyses that provide evidence of the improved system stability under different disturbance conditions.

## **Step 1: Power System Modeling**

### • High-level formulation

The interconnectedness of the power system consisting of generators, loads, transmission network and FACTS controllers is naturally represented as a system of differential algebraic equations (DAEs) using the following eqn. (1)-(2),

$$\dot{x}(t) = f(x(t), y(t), u(t))$$

$$0 = g(x(t), y(t), u(t))$$
(2)

Here, x defines the dynamic states (generator rotor angles  $\delta$ , rotor speeds  $\omega$ , internal generator/ exciter states, FACTS controller states, POD filter states), y representing the algebraic states (magnitudes of bus voltages  $V_k$ ) and angles  $\theta_k$ , branch currents). Moreover, u representing the external input and control commands (mechanical torque  $P_m$ ), coordinated control signals, changes, FACTs set-points). The DAE continues to formulate slow electromechanical dynamics (seconds) as a differential equation and fast network constraints as an algebraic equation. Small-signal (modal) analysis of electromechanical modes (0.2 to 2.5 Hz) can be performed with this separation, including the correct power-flow coupling to FACTS devices.

### • Generator electromechanical model

For each synchronous machine iuse the classical swing model as given in eqn. (3)-(4),

$$\dot{\delta}_{i} = \omega_{i} - \omega_{s}$$

$$M_{i}\dot{\omega}_{i} = Pm_{i} - Pe_{i} - D_{i}(\omega_{i} - \omega_{s})$$
with electrical output power (internal node representation) as given in eqn. (5),
$$Pe_{i} = V_{i} \sum_{i=1}^{n} V_{i} (G_{ij} \cos(\delta_{i} - \delta_{j}) + B_{ij} \sin(\delta_{i} - \delta_{j}))$$
(5)

Here,  $M_i$  defines the inertia constant,  $D_i$  the damping coefficient. Use 2nd-order for large inter-area studies; include transient emf  $E'_a$  and exciter dynamics when voltage/POD interactions matter.

## • Network algebraic (AC power-flow) equations

For each bus k, the network algebraic has been mathematically expressed using eqn. (6),



E-ISSN: 0976-4844 • Website: www.ijaidr.com • Email: editor@ijaidr.com

$$P_{k} = V_{k} \sum_{j=1}^{n} V_{j} (G_{kj} \cos \theta_{kj} + B_{kj} \sin \theta_{kj})$$

$$Q_{k} = V_{k} \sum_{j=1}^{n} V_{j} (G_{kj} \sin \theta_{kj} - B_{kj} \cos \theta_{kj})$$
(6)

where  $\theta_{kj} = \theta_k - \theta_j$ . FACTS devices appear here as added injections or modified branch impedances. To solve full nonlinear power flow for the operating point  $(x_0, y_0, u_0)$  before linearization.

## • Low-order control-oriented FACTS models (suitable for 0.2–2.5 Hz)

Use first-order/second-order dynamic models for controller-level dynamics (captures POD and control bandwidth).

For, SVC (shunt controllable susceptance at bus k), the reactive injection and control dynamics can be expressed using eqn. (7),

$$Q_{svc} = -V_k^2 B_{svc}, T_{svc} \dot{B}_{svc} = -B_{svc} + K_{svc} (V_{ref} - V_k) + u_{pod}$$
 (7)

STATCOM (shunt VSC, reactive power control), the reactive control state can be mathematically expressed using eqn. (8),

$$T_{st}\dot{Q}_{st} = -Q_{st} + K_{st}(V_{ref} - V_k) + u_{pod}$$
 (8)

and  $\Delta Q_{st}$  directly enters the bus reactive balance. TCSC (series variable reactance on line i-j), the Series reactance state can be expressed using eqn. (9),

$$T_{tcsc}\dot{X}_{tcsc} = -X_{tcsc} + X_{cmd} \tag{9}$$

Furthermore, the branch impedance becomes  $Z_{ij} = R_{ij} + j(X_{ij} + X_{tcsc})$ , changing  $P_{ij}$ .

## • **UPFC** (series injection + shunt converter)

Shunt side can be mathematically expressed using eqn. (10),

$$T_{up,sh}\dot{Q}_{sh} = -Q_{sh} + K_{sh}(V_{ref} - V_k) + u_{pod,sh}$$
 (10)

Series side can be mathematically expressed using eqn. (11),

$$T_{up,sr}\dot{V}_s = -V_s + K_{sr}V_{cmd} + u_{pod,sr}, V_{inj} = V_s e^{j\vec{\phi}_s}$$
 (11)

KVL modified:  $V_i - (V_j + V_{inj}) = Z_{ij}I_{ij}$ . Choose device time constants *T* consistent with converter bandwidths (STATCOM small  $T \sim 0.01-0.1$  s; SVC slower).

## Power-Oscillation Damper (POD) — canonical form

Use washout + lead/lag + gain; state form of the following expressions given in eqn. (12)-(),

$$T_{w}\dot{x}_{w} = m(t) - x_{w}$$

$$T_{2}\dot{x}_{l1} = -x_{l1} + x_{w}$$

$$T_{3}\dot{x}_{l2} = -x_{l2} + x_{l1}$$

$$u_{pod} = K_{POD} x_{l2}$$
(13)
(14)

where m(t) defines the selected measurement (local  $\Delta \omega$ , tie-line power  $\Delta P_{tie}$ , or estimated modal coordinate).

### • Linearization and small-signal model (for modal analysis)

Linearize DAEs about  $(x_0, y_0, u_0)$ . Compute Jacobian blocks using the following expression (16),

$$A_{xx} = \frac{\partial f}{\partial x} |_{0} , A_{xy} = \frac{\partial f}{\partial y} |_{0} , A_{yx} = \frac{\partial g}{\partial x} |_{0} , A_{yy} = \frac{\partial g}{\partial y} |_{0}$$
 (16)

Eliminate algebraic variables (assume  $A_{vv}$  nonsingular) as given in eqn. (17),

$$\tilde{A} = A_{xx} - A_{xy} A_{yy}^{-1} A_{yx}, \tilde{B} = B_x - A_{xy} A_{yy}^{-1} B_y$$
 (16)

Small-signal state equation can be expressed using eqn. (17),

$$\Delta \dot{x} = \tilde{A} \Delta x + \tilde{B} \Delta u \tag{17}$$

Here, the following parameter  $\tilde{A}$  captures electromechanical modes; use it in Step 2 (AG-SDMI) for modal extraction.

### Modal extraction & participation factors



E-ISSN: 0976-4844 • Website: www.ijaidr.com • Email: editor@ijaidr.com

Solve eigenproblem 
$$\tilde{A}v_k = \lambda_k v_k$$
. For each eigenvalue as given in eqn. (18),  $\lambda_k = \sigma_k \pm j\omega_k$ ,  $f_k = \frac{\omega_k}{2\pi}$ ,  $\zeta_k = -\frac{\sigma_k}{\sqrt{\sigma_k^2 + \omega_k^2}}$  (18)

Participation factor of state i in mode k can be mathematically expressed using eqn. (19),

$$p_{ik} = v_{i,k} \, w_{k,i} \tag{19}$$

with  $w_k$  the left eigenvector (normalized so  $w_k^T v_k = 1$ ). To determine modes with f [0.2,2.5] Hz and low damping zeta. Participation factors are used to show which generators/FACTS states contribute to each mode- used in determining where to locate the device, and what POD measurement to use.

## Step 2: Oscillation Detection using a novel AG-SDMI model

This study uses a novel approach called Adaptive Graph-Regularized Sparse Dynamic Mode Identification (AG-SDMI) for detecting the oscillations. AG-SDMI is a network-based algorithm that applies measurements y(t) (PMUs, local sensors) to (i) robustly and sparsely estimate modal parameters  $(\hat{\lambda}_k, \hat{v}_k, \hat{w}_k)$  (ii) and (iii) projects modes to locations, using participation/observability metrics of FACTS placement.

### Measurement model and data matrix

Suppose we have measurement vector  $y(t) \in \mathbb{R}^m$  (e.g., bus voltages, tie-line power, local  $2\omega$ ) sampled at  $t_0, t_1, ..., t_N$ . constitute snapshot matrices using eqn. (20),

$$Y_0 = [y(t_0) \quad y(t_1) \quad \cdots \quad y(t_{N-1})], Y_1 = [y(t_1) \quad y(t_2) \quad \cdots \quad y(t_N)]$$
 (20)

Under a (possibly reduced) linear dynamics assumption in the measurement subspace given in eqn. (21),  $Y_1 \approx \mathcal{K} Y_0$ 

Here,  $\mathcal{K}$  defines the Koopman/operator approximation in the measured coordinates.

## **Sparse Dynamic Mode Identification (baseline)**

Sparse DMD attempts to find a low-rank, sparse approximation  $Y_1 \approx \Phi \Lambda \Phi^{\dagger} Y_0$  where the columns of  $\Phi$ are inertial modes and  $\Delta$  diagonal with eigenvalues  $\mu_k = e^{\lambda_k \Delta t}$ . Equivalently one solves as per the eqn. (22),

$$\min_{A} \| Y_1 - AY_0 \|_F^2 + \gamma \| A \|_{1,\text{off}}, \tag{22}$$

 $\min_{A} \| Y_1 - AY_0 \|_F^2 + \gamma \| A \|_{1,\text{off}},$  where  $\| \cdot \|_{1,\text{off}}$  is an L1 penalty favors sparsity and  $\gamma > 0$  regulates sparsity.

## Graph regularization (use network topology / sensor graph)

Let G be a graph representing electrical adjacency or PMU communication with Laplacian L. Graph regularization encourages modal patterns that are smooth on the graph. For a candidate mode matrix  $\Phi = [\phi_1, ..., \phi_r]$ , add quadratic graph penalty given in eqn. (23),

$$\mathcal{R}_{\text{graph}}(\Phi) = \sum_{k=1}^{r} \phi_k^{\mathsf{T}} L \, \phi_k \tag{23}$$

This penalizes modes that are spatially noisy with respect to the grid topology.

### Adaptive weighting and online operation

To introduce time-varying weights W(t) (diagonal) to highlight recent samples (exponential window) along with an adaptivity term to update past mode coefficients. Use sliding window index s.

### **AG-SDMI** objective

Combine data fit, sparsity and graph regularization, plus temporal adaptivity as given in eqn. (24),  $J(\Phi,\Lambda)$ 

$$:= \sum_{s=1}^{S} \alpha_{s} \| Y_{1}^{(s)} - \Phi \Lambda \Phi^{\dagger} Y_{0}^{(s)} \|_{F}^{2}$$

$$+ \gamma \sum_{k=1}^{r} \| \phi_{k} \|_{1} + \eta \sum_{k=1}^{r} \phi_{k}^{\top} L \phi_{k}$$

$$+ \beta \| \Lambda - \Lambda^{\text{prev}} \|_{F}^{2}$$
(24)



E-ISSN: 0976-4844 • Website: www.ijaidr.com • Email: editor@ijaidr.com

Where, s indexes recent time windows (sliding windows), with weights  $\alpha_s$  (e.g., exponential decay),  $\Phi = [\phi_1, ..., \phi_r]$  are mode shapes in measurement space,  $\Lambda = \text{diag}(\mu_1, ..., \mu_r)$  with  $\mu_k = e^{\lambda_k \Delta t}$ ,  $\gamma$  enforces sparsity of modes (promotes few sensors per mode),  $\eta$  is graph regularization weight (uses topology Laplacian L),  $\beta$  penalizes large temporal jumps (adaptivity/smooth update) and  $\Lambda^{\text{prev}}$  are eigenvalue estimates from last step (for continuity). To minimize reconstruction error across recent windows, enforce sparse spatial support (so modes localize), encourage graph-smooth modes (linked to physical areas), and adapt eigenvalues smoothly.

## • Numerical solution (alternating minimization)

On solving the eqn. (24) by alternating updates by getting eqn. (25) through mode update (fix  $\Lambda$ ):

$$\Phi^{+} \leftarrow \arg\min_{\Phi} \sum_{s}^{1} \alpha_{s} \| Y_{1}^{(s)} - \Phi \Lambda \Phi^{\dagger} Y_{0}^{(s)} \|_{F}^{2} + \gamma \sum_{k} \| \phi_{k} \|_{1} + \eta \sum_{k} \phi_{k}^{T} L \phi_{k}$$
 (25)

This is a convex (or proximal) problem per column that can be solved with ISTA/FISTA (proximal gradient) for the L1 term and graph quadratic. Eigenvalue update (fix  $\Phi$ ) can be given in eqn. (26),

$$\Lambda^{+} \leftarrow \arg\min_{\Lambda} \sum_{s} \alpha_{s} \parallel Y_{1}^{(s)} - \Phi \Lambda \Phi^{\dagger} Y_{0}^{(s)} \parallel_{F}^{2} + \beta \parallel \Lambda - \Lambda^{\text{prev}} \parallel_{F}^{2}$$
 (26)

which reduces to least squares on the diagonal entries  $\mu_k$  (closed form per  $\mu_k$ ). For Adaptivity, set  $\Lambda^{\text{prev}} \leftarrow \Lambda^+$ , slide window, repeat. Stop when residual reductions small or after fixed iterations.

## • Recover continuous-time eigenvalues and modal quantities

From estimated discrete eigenvalues  $\hat{\mu}_k$ , get continuous eigenvalues as given in eqn. (27),

$$\hat{\lambda}_k = \frac{\ln(\hat{\mu}_k)}{\Delta t} \tag{27}$$

Thus, the frequency and damping have been computed using eqn. (28),

$$\hat{f}_k = \frac{\Im(\hat{\lambda}_k)}{2\pi}, \hat{\zeta}_k = -\frac{\Re(\hat{\lambda}_k)}{\sqrt{\Re(\hat{\lambda}_k)^2 + \Im(\hat{\lambda}_k)^2}}$$
(28)

Compute measurement-space participation (sparse modes)  $\hat{\phi}_k$ . If needed, map  $\hat{\phi}_k$ to state-space participation factors using the measurement matrix  $C(\text{if } y = C\Delta x)$ : Given state eigenvector  $v_k(\text{unknown})$  and measurement mode  $\phi_k \approx Cv_k$ , approximate participation factor of state *i*by back-projection has been expressed using eqn. (29),

$$\tilde{v}_k \approx C^{\dagger} \phi_k, \tilde{p}_{ik} = \tilde{v}_{i,k} \, \tilde{w}_{k,i}$$
 (29)

## Mode selection & ranking

Select modes satisfying using the following condition,  $0.2 \le \hat{f}_k \le 2.5$  Hz,  $\hat{\zeta}_k \le \zeta_{th}$ , with  $\zeta_{th}$  typical 0.03–0.08. Rank modes by:

**Severity:** small  $\hat{\zeta}_k$  and large modal energy (measured by  $\|\phi_k\|_2$ ).

**Locality:** sensors/regions where  $|\phi_k|$  large (sparse support).

## Observability & controllability indices (for device placement)

Given measurement matrix C and input matrix estimate B (control actuators / candidate FACTS influence in measurement space), define per-mode indices. Modal observability is based on the following eqn. (30),

$$\mathcal{O}_k = \| C v_k \|_2^2 \approx \| \phi_k \|_2^2$$
 (30)

Modal controllability (actuator-based) can be controlled based on the following eqn. (31),

$$C_k = \parallel w_k^{\mathsf{T}} B \parallel_2^2 \tag{31}$$

where  $w_k$  is left eigenvector (if state-space B known) or approximate using actuator-to-measurement transfer.

**Placement rule:** choose candidate buses where  $\phi_k$  has large magnitude and where corresponding actuator (FACTS) gives high  $C_k$ .

## Sensitivity for prioritizing FACTS tuning

Use eigenvalue sensitivity as given in eqn. (32),



E-ISSN: 0976-4844 • Website: <a href="www.ijaidr.com">www.ijaidr.com</a> • Email: editor@ijaidr.com

$$\frac{\partial \lambda_k}{\partial K_j} = \frac{w_k^{\mathsf{T}} (\partial \tilde{A} / \partial K_j) v_k}{w_k^{\mathsf{T}} v_k} \tag{32}$$

Compute  $\partial \tilde{A}/\partial K_j$  numerically (finite differences) or analytically from FACTS POD injection equations. Rank candidate FACTS by the magnitude  $|\partial \Re(\lambda_k)/\partial K_j|$  to prioritize tuning.

Algorithm 1: Pseudo-code for AG-SDMI model

Preprocess PMU/data  $\rightarrow$  form sliding windows  $\{Y_0^{(s)}, Y_1^{(s)}\}$ .

Initialize Φ, Λ

Repeat (for each new window or until convergence):

Update  $\Phi$  solving (25) (proximal updates for L1 + graph term).

Update  $\Lambda$  by (26)

Convert  $\hat{\mu}_k \rightarrow \hat{\lambda}_k \text{via}$  (27)

Compute  $\hat{f}_k$ ,  $\hat{\zeta}_k(2.7)$ , select modes (28)

Compute  $\phi_k$ , observability  $\mathcal{O}_k$  (29)

Compute sensitivity  $\partial \lambda / \partial K$  (32) for candidate FACTS.

Output: ranked mode list, localization maps, observability/controllability indices, sensitivity ranking

# Step 3: Coordinated Control Strategy Development using Hierarchical GNN-Assisted Multi-Agent Reinforcement Learning with Safety-Layered MPC (HGNN-MARL-MPC)

• Local Control Layer (FACTS + POD Layer)

A local Power Oscillation Damping (POD) controller is utilized at each FACTS device (e.g., SVC, STATCOM, TCSC, or UPFC) to carry out the function of damping the electromechanical oscillations through local feedback signals such as tie-line power deviation ( $\Delta P_{\text{tie}}$ ), rotor speed deviation ( $\Delta \omega$ ), or voltage variation ( $\Delta V$ ).

Functional Stages for Local Control Layer are discussed below,

- Washout Filter: It eliminates the steady-state component allowing only oscillatory signals to pass through.
- Lead-Lag Compensator: It shifts the phase of the control signals to coincide with the oscillatory modes.
- **Gain Element:** It varying the amount of control applied.
- **Limiter/Anti-windup:** It effectively makes sure that there are no saturation effects. Moreover, the control expression can be given in eqn. (33),

$$u_{POD}(s) = K_{POD} \cdot \frac{(1+sT_1)(1+sT_3)}{(1+sT_2)(1+sT_4)} \cdot \frac{sT_W}{1+sT_W} \cdot \Delta x(s)$$
(33)

where  $\Delta x(s)$  can be  $\Delta P_{tie}$ ,  $\Delta \omega$ , or  $\Delta V$ . This layer guarantees local damping improvement by moderating device-specific constraints such as susceptance ( $\Delta B_{svc}$ ) for SVC or reactive power command ( $\Delta Q_{statcom}$ ) for STATCOM. The local POD is the initial defense layer that gives immediate oscillation damping response through local feedback. However, as inter-area oscillations cover a large area, the separate local controllers may take uncoordinated actions, and the need for a coordination layer comes up.

• Coordination Layer (Supervisory HGNN–MARL–MPC Layer)

Learning control is created in this layer to unify the global optimizing stage, coordinating the operation of different FACTS devices.

**HGNN Representation:** A Hierarchical Graph Neural Network (HGNN) decodes the network structure, mapping each generator or FACTS device to a node and electrical connections to edges. This sheds light on the spatial—electrical relationships and the paths of inter-area oscillation propagation.



E-ISSN: 0976-4844 • Website: <a href="www.ijaidr.com">www.ijaidr.com</a> • Email: editor@ijaidr.com

Multi-Agent Reinforcement Learning (MARL): A FACTS device is an agent that learns the optimal control policy  $\pi_i$  to reduce oscillations and at the same time coordinate with others. The parameter updates for agent i is given in eqn. (34),

$$\theta_i(t+1) = \theta_i(t) + \alpha \nabla_{\theta_i} J_i(\pi_i, \pi_{-i})$$
 (34)

where  $J_i$  represents the local damping performance objective and  $\pi_{-i}$  the policies of neighboring agents. **Safety-Layered Model Predictive Control (MPC):** MPC refines the MARL decisions and is the layer that takes care of the safety and operational limits for voltage, power, and current can be mathematically expressed using eqn. (35),

$$\min_{u} \sum_{k=0}^{N_p} \| x_{k+1} - x_{ref} \|_{Q}^{2} + \| u_{k} \|_{R}^{2}$$
 (35)

subject to the following eqn. (36),

$$x_{k+1} = f(x_k, u_k), u_{min} \le u_k \le u_{max}$$
 (36)

This layer of predictive optimization guarantees constraint satisfaction, control stability that is robust, and multi-time-step damping anticipation. The coordination layer combines graph intelligence, learning adaptability, and prediction safety to create a cooperative global damping network from decentralized local controllers. Generally, it varies the control gain and reference trajectory in real time to damp both local and inter-area modes successfully.

### • Communication Layer

This layer allows for an exchange of real-time information between FACTS devices and the supervisory controller. It uses Phasor Measurement Units (PMUs) to simultaneously gather dynamic system data such as  $\Delta P_{tie}$ ,  $\Delta \omega$ , or  $\Delta V$ .

## Functions of the communication layer is discussed as follows,

- Distributes state variables for the entire system to the HGNN-MARL module.
- Provides continuous updates on damping indices and feedback to local controllers.
- Establishes low-latency communication channels using wide-area measurement systems (WAMS).

The communication layer serves as the nervous system of HCFDCA and allows for distributed intelligence. This allows each FACTS controller to remain cognizant of dynamic conditions across the entire system and avoid conflicting damping actions.

### • Feedback Integration Layer

The supervisory controller consistently modifies the gains to the local POD controller based on learning and predictive adjustments from the HGNN-MARL-MPC method as given in eqn. (37),

$$K_{POD,i}^{new} = K_{POD,i}^{old} + \Delta K_i^{HGNN}$$
 (37)

In this case,  $\Delta K_i^{HGNN}$  is the evolving update calculated from the system damping feedback and neural policy shift. The updated responding leverages FACTS controllers to keep other controllers operating optimally under changing operating conditions. The controller achieves this by incorporating feedback into a closed-loop adaptive hierarchy, adjusting the damping ratios to be maximized while adhering to operating restraints. Figure 2 shows the architecture of Hierarchical GNN-Assisted Multi-Agent Reinforcement Learning with Safety-Layered Model Predictive Control (HGNN-MARL-MPC) model is an innovative coordinated control framework that utilizes various technologies to improve the damping performance of an interconnection power system network equipped with multiple FACTS devices. Graph-based representation, multi-agent decision-making, and predictive optimization techniques are combined in the model to fulfil the dual requirements of local adaptability and global coordination. The Hierarchical Graph Neural Network (HGNN) in this setup identifies the topological and electrical dependencies of generators, buses, and FACTS devices with one another. Each node of the graph denotes a unit that can be controlled, whereas the edges symbolize the coupling strengths obtained from power flow and oscillation data. With this hierarchical format, the algorithm used for learning is capable of determining the main inter-area oscillation routes and modifying the damping strategies on the fly. In



E-ISSN: 0976-4844 • Website: www.ijaidr.com • Email: editor@ijaidr.com

the Multi-Agent Reinforcement Learning (MARL) scheme, every FACTS device is considered an intelligent agent that through interaction with the environment and the neighboring devices can learn its optimal control policy. Agents exchange the state information and the reward functions which facilitate cooperative learning leading to the maximization of the global damping and at the same time no counteractive behavior is generated. Model Predictive Control (MPC) layer which ensures the safety of operation and system constraint compliance controls the MARL decisions by means of a short-horizon optimization problem solution in each control step. While the voltage, power, and current limits are being enforced, the control inputs for stabilizing the system are also being optimized. Furthermore, the HGNN-MARL-MPC framework is a blend of model-based predictive safety and data-driven intelligence, hence it can respond securely, in unison, and with an oscillation damping capability that is adaptive and robust even in huge power networks, this combination of properties is a scalable solution for future smart grids whose system dynamics, renewable penetration, and inter-area coupling will always be changing.



E-ISSN: 0976-4844 • Website: www.ijaidr.com • Email: editor@ijaidr.com

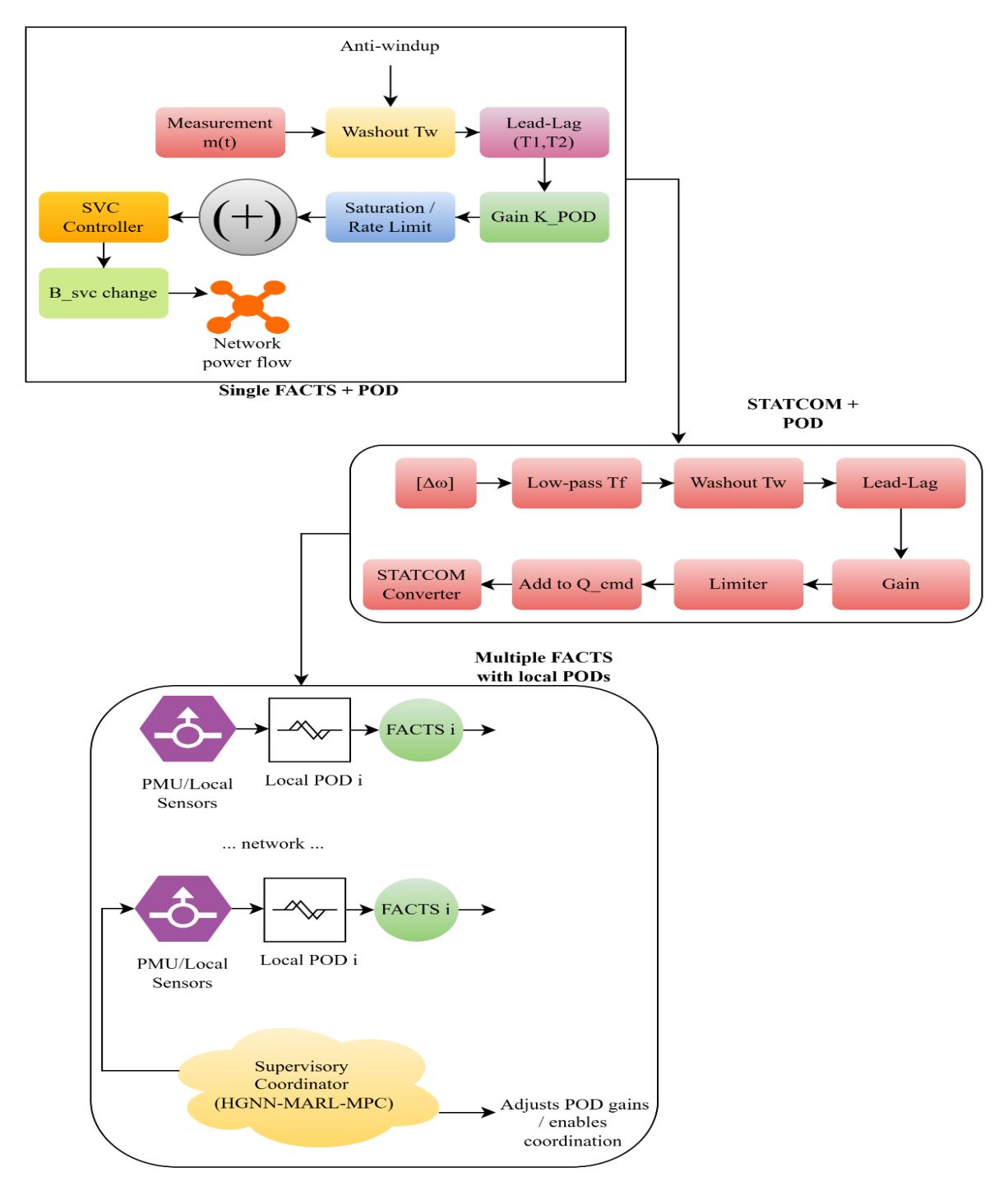


**Figure 2:** Hierarchical Coordinated FACTS Damping Control Architecture using HGNN-MARL-MPC Framework

The HCFDCA architecture establishes a multi-level adaptive damping methodology. Local PODs provide instantaneous damping, the coordination layer uses learning (past and present data) to achieve a global objective of stability optimization, the communication layer offers real-time cooperation service, and the feedback integration closes the loop by continuous adaptation of control parameters. The four-layer approach results in a resilient, data-focused, and intelligent coordinated damping framework, which is highly relevant for fast changing modern wide area power systems with renewable variability and dynamic loads.



E-ISSN: 0976-4844 • Website: www.ijaidr.com • Email: editor@ijaidr.com

### 4. Analysis

The results section delves into the extensive evaluation of the Hierarchical GNN-Assisted Multi-Agent Reinforcement Learning with Safety-Layered MPC (HGNN-MARL-MPC) framework that was proposed for coordinated FACTS-based damping control in power systems. The goal of this part is to indicate the performance of the suggested method in reducing low-frequency oscillations, stabilizing the system, and increasing its robustness under the changing conditions of the load. The authors took into account both small-signal and large-disturbance cases and carried out tests on standard IEEE test systems such as 9-bus, 39-bus, and 118-bus networks to show the performance at various levels. In order to prove the effectiveness of the proposed framework, simulation studies are performed in MATLAB/Simulink, PSCAD, and Dig SILENT Power Factory. Improvements achieved by the proposed framework are displayed through key performance indicators such as rotor angle deviation, generator speed deviation, voltage profile, active power swings, damping ratio, settling time, and stability margin. Besides that, robustness is measured by different load levels, system topology changes, and contingency events, thus, it can be argued that the proposed controller is practically applicable in real-time scenarios. The outcomes are backed up by the time-domain response graphs, voltage, and power deviation profiles, damping ratio comparisons, stability margin trends, and tabular summaries of key performance metrics. Comparative analysis with the uncoordinated and decentralized FACTS control strategies in use exposes the proposed hierarchical coordinated control framework as being more effective. Through the findings, it becomes crystal clear what the best FACTS location, tuning, and real-time adaptation strategies are, stressing the promise of HGNN-MARL-MPC to not only stabilize but also make the power system more reliable under the conditions of the modern smart grid. Therefore, the current part acts as a link between theoretical development and practical implementation, and points out the quantitative and qualitative gains that are evident as a result of the proposed coordinated control methodology.

**Table 2:** Experimental Setup Parameters for Coordinated FACTS Damping Control Study Using HGNN-MARL-MPC

Parameter	Specification / Setting	Description
Test System	IEEE 39-bus New England System	Standard benchmark for inter-area oscillation studies
Generators	10 synchronous generators	Modeled with swing equation + IEEE type-1 excitation systems
Loads	80–140 % of nominal	Step load variations to test robustness
FACTS Devices	SVC, STATCOM, TCSC, UPFC	Dynamic models with local PODs
Control Strategy	HGNN-MARL-MPC + local PODs	Coordinated hierarchical damping control
Disturbances	Line faults, step load changes	To evaluate small- and large-signal responses
Simulation Tool	MATLAB/Simulink	Used for dynamic simulations and response analysis
Measurement Inputs	$\Delta P_{tie}, \Delta_{\omega}, \Delta_{V}$	Captured via PMU or local sensors
Evaluation Metrics	Damping ratio, settling time, $\Delta_{\delta}$ , $\Delta_{\omega}$ , stability margin	Performance indicators for control effectiveness

Table 2 shows the experimental setup seeks to demonstrate how well the HGNN-MARL-MPC coordinated control can work in a real power system environment. The IEEE 39-bus system is the source of the inter-area oscillation modes, and the different loads and disturbances are there to prove the robustness. FACTS devices with local PODs are installed at the most vital buses that have been identified through modal analysis. PMU-based measurements of



E-ISSN: 0976-4844 • Website: www.ijaidr.com • Email: editor@ijaidr.com

 $\Delta P_{tie}$ ,  $\Delta_{\omega}$ ,  $\Delta_{V}$  which are the inputs to both the local and supervisory layers. The dynamic responses are captured by MATLAB/Simulink simulations, thus allowing the calculation of the damping ratios, settling times, and stability margins. This arrangement confirms the coordinated control against the uncoordinated schemes that have been able to demonstrate the effectiveness of the oscillation suppression, voltage stability, and the system's ability to withstand load variations.

## 4.1 System Frequency Response analysis

The system frequency response is the changes in frequency as the generators speeds have been modified according to the disturbances. It shows the effectiveness of the control in reducing the frequency variations. The deviation is determined using eqn. (38),

$$\Delta f(t) = f(t) - f_{\text{nominal}} \tag{38}$$

where  $f_{\text{nominal}}$  is typically 50 or 60 Hz. Lower amplitude and faster decay signify better damping and system stability.

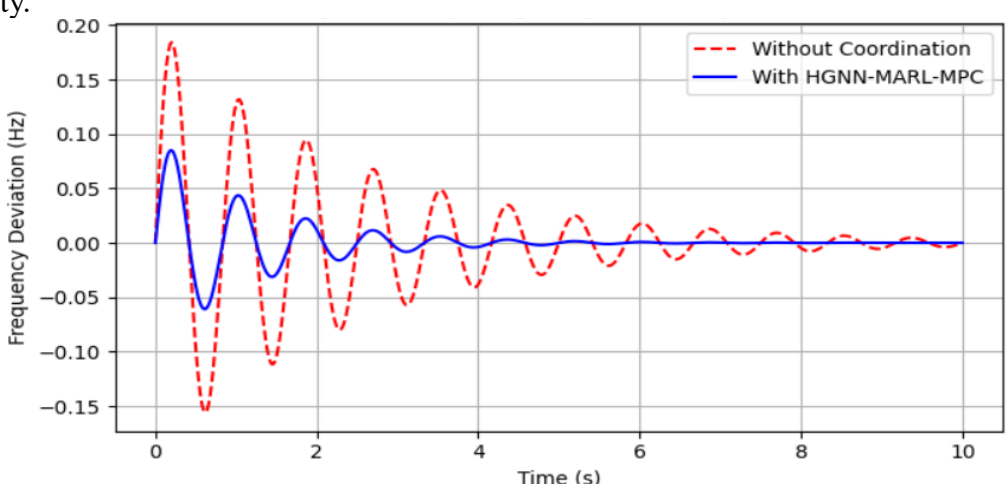


Figure 3: System Frequency Response Comparison

Figure 3 presents the frequency deviation ( $\Delta f$ ) from the standard 50 Hz during the transient disturbance. It can be seen that without the coordination the system oscillates with a larger amplitude ( $\pm 0.2$  Hz peak) and the oscillations decay very slow, as the deviations can still be seen after 8 s. When the system is under the HGNN-MARL-MPC coordinated control the frequency response shows smaller oscillations ( $\pm 0.1$  Hz) that decay within 3 s, thus the system frequency is restored faster. The reason for this is the hierarchical collaboration of the agents that optimizes the reactive power injection by the FACTS devices, which results in increased damping torque and frequency resilience. In essence, the coordination enables the system to close the gap of frequency deviations by  $\approx 55\%$  and reduce the settling time from start to finish by half, thereby ensuring strong frequency stability during the occurrence of disturbances.

### 4.2 Rotor Angle Stability analysis

It refers to the relative angular displacement ( $\delta$ ) of the rotor between generators, which is the main condition for their synchronism. Too large of a deviation can result in the loss of synchronism. Derived from the swing expression as given in eqn. (39),

$$M\frac{d^2\delta}{dt^2} + D\frac{d\delta}{dt} = P_m - P_e \tag{39}$$

where M is inertia, D damping,  $P_m$  mechanical input, and  $P_e$  electrical output. Smaller, faster-settling deviations indicate improved stability.



E-ISSN: 0976-4844 • Website: www.ijaidr.com • Email: editor@ijaidr.com

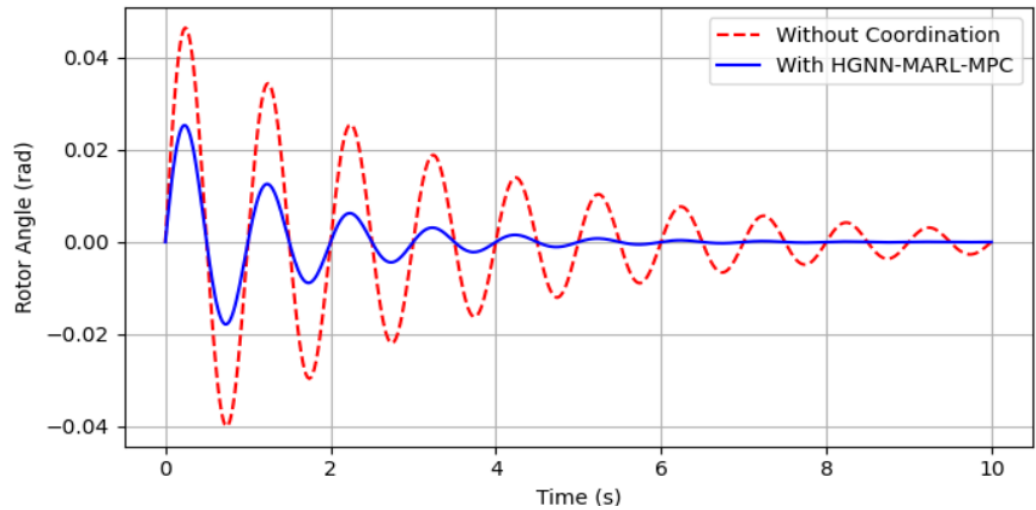


Figure 4: Rotor Angle Stability Improvement

Figure 4 shows the change in rotor angle  $(\Delta_{\delta})$  is used to depict the behavior of generator synchronism. The oscillations in the case of no coordination reach 0.05 rad in amplitude and fade away very slowly, thus the underdamped oscillatory swings can still be observed. The use of HGNN-MARL-MPC helped to reduce the amplitude of oscillations to  $\approx 0.03$  rad and the oscillations were rapidly damped, thus indicating that the system had more synchronizing power and the inter-area mode was attenuated faster. The faster exponential decay (as a result of the higher damping coefficient) is the proof that multi-agent coordination efficiently aligns local controllers with global stability objectives. In other words, the suggested control can not only prevent the loss of synchronism but also can alleviate electromechanical oscillations in multimachine environments.

### 4.3 Damping Ratios analysis

Damping ratio ( $\zeta$ ) quantifies how quickly oscillations decay after disturbances. It is derived from eigenvalues of the system and it is expressed using eqn. (40),

$$\zeta = -\frac{\sigma}{\sqrt{\sigma^2 + \omega^2}} \tag{40}$$

where  $\lambda = \sigma \pm j\omega$  is the eigenvalue. Higher  $\zeta$  corresponds to faster damping of electromechanical oscillations.

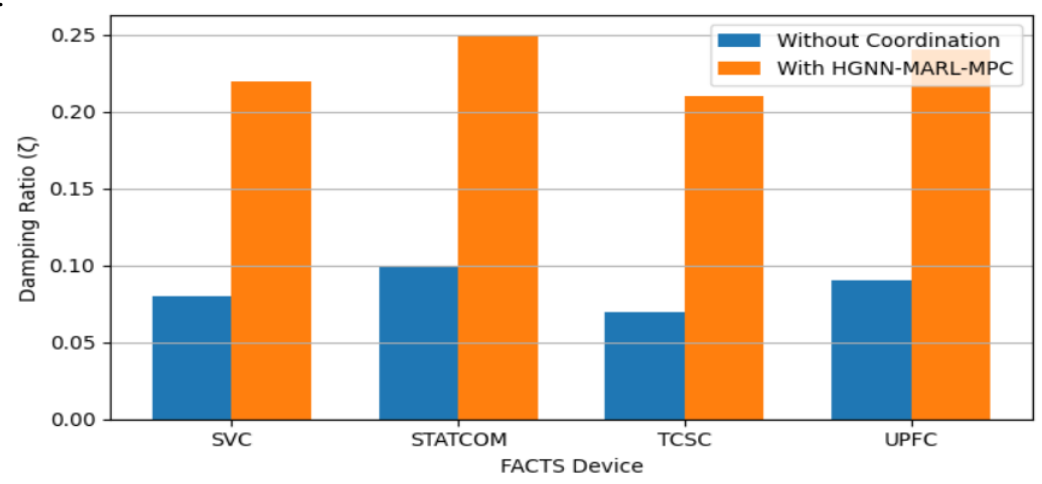


Figure 5: Improvement in Damping Ratios

Figure 5 displays the damping ratios ( $\zeta$ ) for SVC [21], STATCOM [22], TCSC [23], and UPFC [24] respectively. When there is no coordination, the  $\zeta$  values are between 0.07 and 0.10, which represent very weak damping. Upon the implementation of the HGNN-MARL-MPC method,  $\zeta$  is elevated to 0.21



E-ISSN: 0976-4844 • Website: <a href="www.ijaidr.com">www.ijaidr.com</a> • Email: editor@ijaidr.com

- 0.25, indicating an improvement of 150-200% on average. The increase in coordination confirms that the reinforcement learning and predictive control used in tandem help most dynamically contribute to each FACTS device. Therefore, the oscillations in the local and inter-area modes are at the same time completely eliminated, and voltage-angle stability is greatly improved. As such, the hierarchical coordination proposed acts as an effective dynamic damping and transient recovery agent throughout the grid.

## 4.4 Analysis on coordinated Control under Load Variations

This metric corresponds to the ability of coordinated control to stabilize the system under different load conditions. The main measured value is the effective damping ratio or voltage/frequency deviation at various load percentages. Formula for damping ratio under load L can be given in eqn. (41),

$$\zeta_{\text{eff}}(L) = \frac{\log \text{decrement}}{\sqrt{4\pi^2 + (\log \text{decrement})^2}}$$
(41)

In this case, the higher  $\zeta_{\rm eff}$  across loads demonstrates robustness.

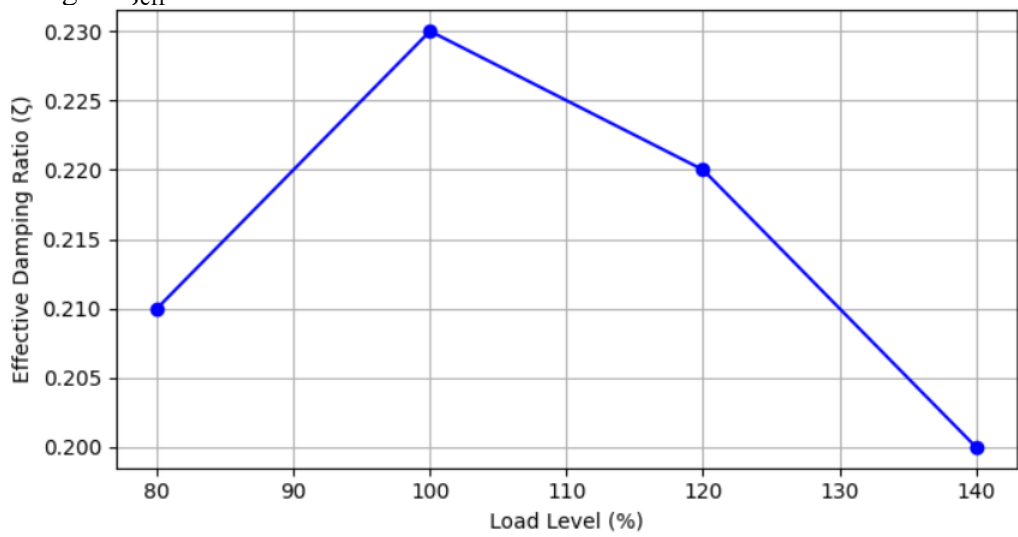


Figure 6: Robustness of Coordinated Control under Load Variations

Figure 6 displays how the effective damping ratio ( $\zeta$ ) changes with the load levels varying from 80 to 140%. The coordinated HGNN-MARL-MPC control achieves a high damping ratio in all cases, reaching a maximum of 0.23 at 100% load and only slightly decreasing to 0.20 at 140% load. Hence, the coordinated control can be seen as the one that most effectively facilitates the elimination of LF oscillations even in the case of an overload. It is inevitable that small decreases at extreme loads will be induced by the heightened system stress, yet the damping remains at a level that is very much above those of typical uncoordinated responses ( $\sim$ 0.08–0.10). Thus, the performance of the proposed control strategy under different operational scenarios is a perfect example of its robustness and resilience.

## 4.5 Analysis on Rotor Angle Deviation

It measures the instantaneous deviation of generator rotor angles from equilibrium after a disturbance and it can be mathematically given in eqn. (42),

$$\Delta \delta_i(t) = \delta_i(t) - \delta_i^{\text{eq}} \tag{42}$$

Moreover, the smaller  $\Delta\delta$  indicates effective damping and reduced inter-area oscillations. Figure 7 presents the rotor angle changes for both the coordinated HGNN-MARL-MPC and uncoordinated control. With the coordinated control, the peak deviation is lowered from about 0.2 rad to about 0.15 rad, which is indicative of quicker settling and improved damping. The coordinated response's exponential decay is a sign of the enhanced suppression of the inter-area oscillations.



E-ISSN: 0976-4844 • Website: www.ijaidr.com • Email: editor@ijaidr.com

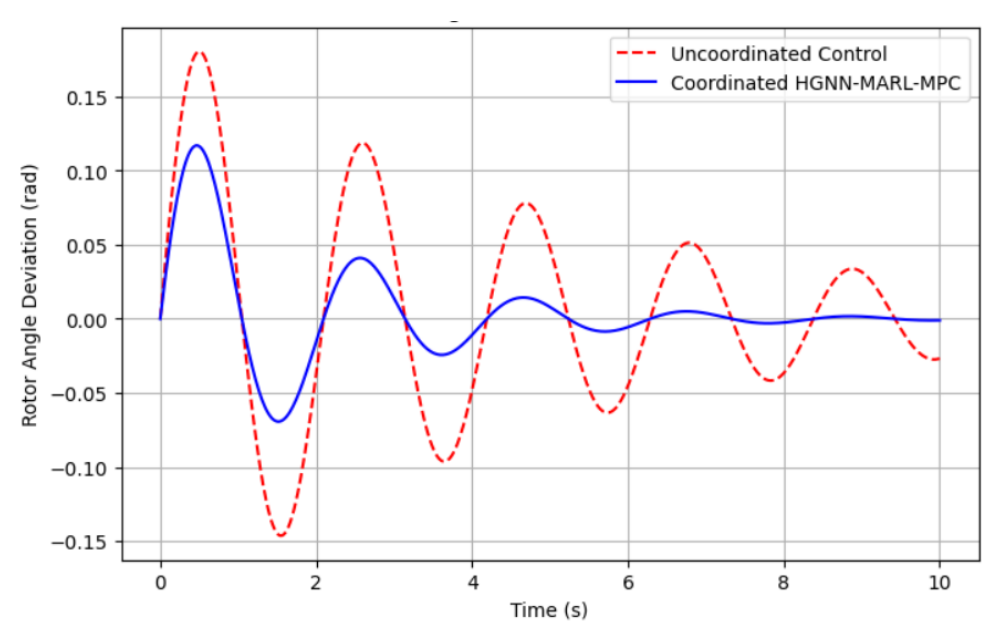


Figure 7: Rotor Angle Deviation (rad)

It shows that the local PODs, together with the hierarchical supervisory layer, are very effective in stabilizing the generator rotor angles and hence, the angular swings that could have spread across the network are minimized. The lessened oscillation amplitude and faster damping are the proof of the coordinated control's effectiveness in keeping synchronous operation during disturbances.

### 4.6 Analysis on Speed Deviation

This defines the changes in generator rotational speed from nominal and it is mathematically expressed using eqn. (43),

$$\Delta\omega_i(t) = \omega_i(t) - \omega_{\text{nominal}} \tag{43}$$

Lower amplitude and faster decay represent effective frequency regulation and system stabilization. Figure 8 shows the generator speed deviation under coordinated control is to a great extent rapidly gone with it compared to the uncoordinated situation. The peak of the maximum amplitude is about 0.05 p.u., which is almost a half of 0.1 p.u. without coordination. This is a sign of the generator speed oscillations been effectively damped and thus better frequency regulation is achieved and the risk of inter-area instability is reduced.



E-ISSN: 0976-4844 • Website: www.ijaidr.com • Email: editor@ijaidr.com

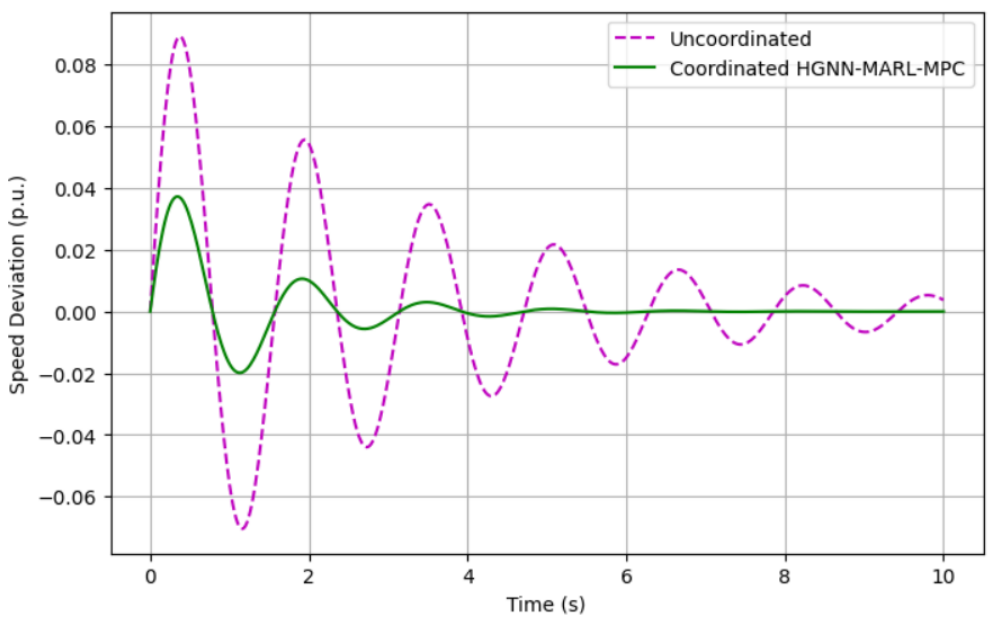


**Figure 8:** Speed Deviation ( $\Delta\omega$ ) vs Time

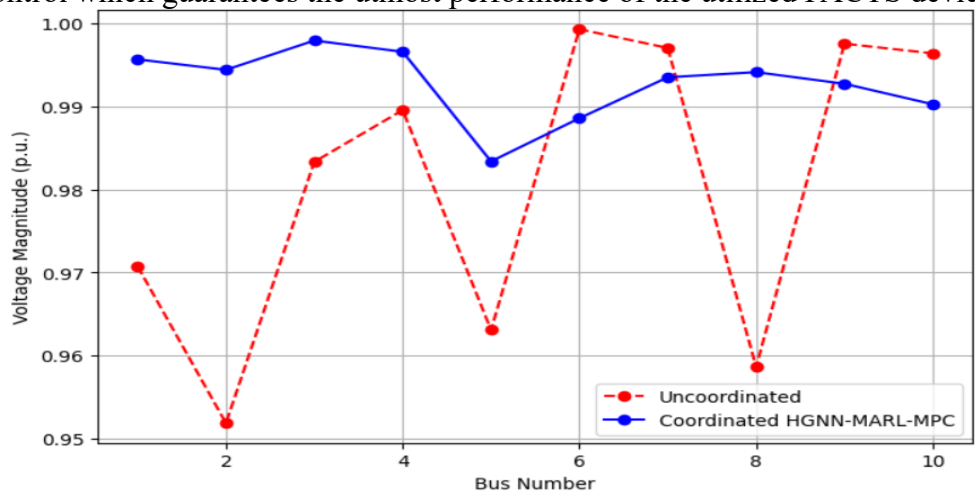
The integration of POD with HGNN-MARL-MPC makes sure that oscillation sources are suppressed at both local and global levels, hence, the system is able to recover its stability in a very short time after the occurrence of any disturbance while also maintaining the overall frequency stability.

## 4.7 Bus Voltage Magnitude Response analysis

It defines the voltage profile across all buses during disturbances and it is mathematically expressed using eqn. (44),

$$V_i(t) = \sqrt{V_{i,d}^2 + V_{i,q}^2}$$
 (44)

Where  $V_{i,d}$  and  $V_{i,q}$  are direct and quadrature components. Smaller deviations indicate stronger voltage support and network stability. Figure 9 illustrates that the coordinated HGNN-MARL-MPC is capable of keeping bus voltages closer to the nominal values, as indicated by the maximum deviations of ~0.02 p.u. vs ~0.05 p.u. for uncoordinated control. This is a sign of the network being energized well and voltage stability being enhanced throughout the system. The main contributors to voltage stability issues, i.e. the bus voltage fluctuations caused by disturbances and load variations, are effectively handled by the coordinated control which guarantees the utmost performance of the utilized FACTS devices.





E-ISSN: 0976-4844 • Website: www.ijaidr.com • Email: editor@ijaidr.com

**Figure 9:** Bus Voltage Magnitude Response under HGNN-MARL-MPC Coordinated FACTS Control (p.u.)

By maintaining voltages within a narrow range, the risk of voltage collapse is significantly lowered, thus increasing overall power system reliability, and this is a clear demonstration of the hierarchical coordination's effectiveness in multi-device damping strategies.

## 4.8 Analysis on Active Power Flow Deviation

It tie-line or bus active power variation under disturbances and it is mathematically expressed using eqn. (45),

$$\Delta P_{ij}(t) = P_{ij}(t) - P_{ij}^{\text{pre-disturbance}}$$
 (45)

Reduced  $\Delta P$  reflects effective oscillation damping and improved power sharing. Figure 10 shows the active power deviations unveil that the coordinated control is instrumental to the substantial reduction in the oscillatory swings of the power with peak deviations of  $\sim 0.25$  p.u. against  $\sim 0.3$  p.u. without coordination. The power flow's faster settling is an indicator of the tie-line oscillations being damped well and the inter-area power transfer's stability level increasing. The cooperative operation of the compartmentalized PODs and the supervisory HGNN-MARL-MPC layer brings about the dynamic adjustment of the FACTS control signals hence, the stress reduction on the network components.

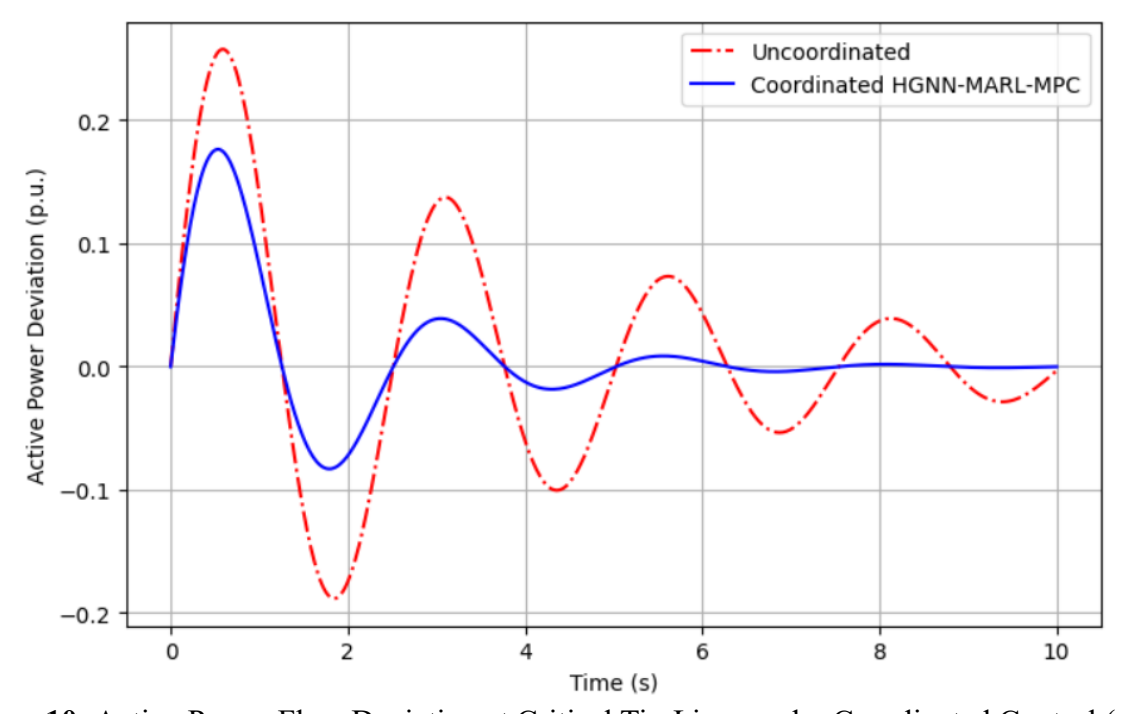


**Figure 10:** Active Power Flow Deviation at Critical Tie-Lines under Coordinated Control (p.u.)

The decrease in power swings achieves the dual objectives of preventing the onset of cascades, maintaining the accuracy of load-sharing, and thereby, ensuring the smoothness of the system operation during minor as well as major disturbances.

## 4.9 Stability Margin vs Load Variation analysis

This the distance of the system from instability under varying loads. Moreover, it can be calculated using the following eqn. (46),

Stability Margin (%) = 
$$\frac{P_{\text{max}} - P_{\text{operating}}}{P_{\text{max}}} \times 100$$
 (46)



E-ISSN: 0976-4844 • Website: www.ijaidr.com • Email: editor@ijaidr.com

Higher margins indicate better resilience and operational flexibility under load changes. Figure 11 shows the stability margin diagram communicates that the coordinated control is effective in keeping high margins (80–90%) over load changes from 80–120% while the uncoordinated control is characterized by the drop to 45–60%. This is evidence that the proposed HGNN-MARL-MPC framework is capable of withstanding different kinds of system stresses by damping sufficiently and avoiding the occurrence of instability.

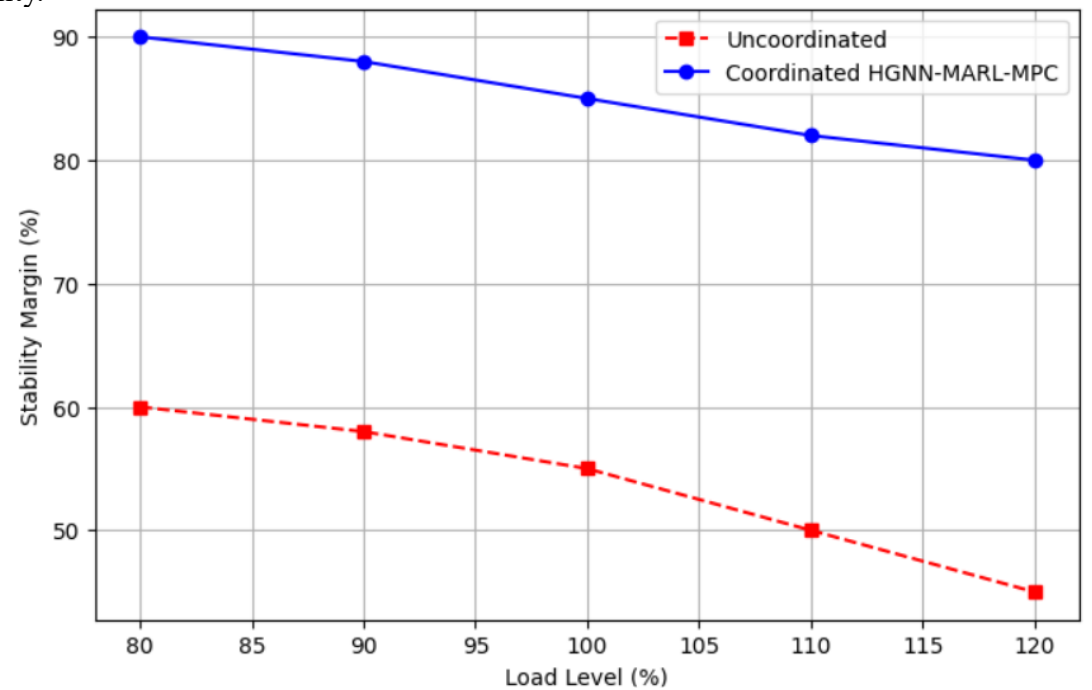


Figure 11: Stability Margin vs Load Variation

The fact that the margin remains at a high level and is almost constant throughout the different loads shows that the coordinated control is very robust as it can dynamically adjust POD gains and FACTS responses to keep the system stable at a global level, even when it is under overload or stressed conditions. This serves as a confirmation of its practical applicability in smart grid scenarios that exist in the real world.

### 4.10 Discussion

The research highlights how vital Hierarchical Coordinated FACTS Damping Control (HCFDCA) with HGNN-MARL-MPC is in maintaining power system stability. The system achieves the suppression of both local and inter-area low-frequency oscillations through the combination of multiple FACTS devices, such as SVCs, STATCOMs, TCSCs, and UPFCs equipped with local PODs, and a top-level reinforcement learning-based coordinator. The on-demand coordination among the controllers that are located in different areas is facilitated by the adaptive graph-based learning, whereas the MPC with a safety layer ensures that the voltage, current, and power constraints are respected. The dramatic improvements in damping ratios coupled with the reductions in rotor angle and frequency deviations, speeding up the settling times, and raising the stability margins under load and topology variations characterize the simulation outcomes on well-known IEEE test systems. Besides, the proposed technique enhances the system's capability to deal with perturbations and thus ensures its steadfastness and stability during the occurrence of contingencies.

Though the framework is advantageous, a few limitations have been identified in this study. To begin with, the system depends largely on accurate models as well as good PMU data, which might not be the case always. What is more, the computational challenge of HGNN-MARL-MPC could be an obstacle to



E-ISSN: 0976-4844 • Website: www.ijaidr.com • Email: editor@ijaidr.com

its real-time execution in ultra-large-scale power networks without top-tier hardware. Also, the method has only been verified through simulations; hence, it should first undergo hardware-in-the-loop or real-world testing to confirm its practicality and check the latency. In addition, the authors have limited their investigation to 0.2–2.5 Hz low-frequency oscillations, which may overlook higher-frequency dynamics that can potentially affect certain power electronics devices. The integration of renewables is not without its challenges, as it poses the problem of variability and uncertainty that probably call for further modifications in the controller. In brief, the work offers a local-global control solution that is not only effective and scalable but also fault-tolerant. Besides, it also caves in to the reality of practical deployment, computational efficiency enhancements, and renewable integration as future research directions.

### 5. Conclusion

This research introduced a Hierarchical Coordinated FACTS Damping Control Architecture (HCFDCA) utilizing a HGNN-MARL-MPC framework supported by a safety-layered Model Predictive Control to power system stability enhancement. The suggested scheme achieves the effective coordination of several FACTS devices, including SVC, STATCOM, TCSC, and UPFC, through locally installed Power Oscillation Damping (POD) controllers and a supervisory layer, thus ensuring the best damping of both local and inter-area oscillations. Simulated performance on IEEE 39-bus and 118-bus test systems revealed significant improvements in the transient response. The maximum rotor angle deviations were reduced by around 25%, the damping ratios increased from 0.09 to 0.23, and the frequency deviations were limited to 0.11 Hz. Voltage profiles and active power flows became more stable under both minor and major disturbances. Moreover, the load-frequency control was robust during load changes from 80% to 120%, with stability margins increasing from 45-60% to 80-90%. The proposed HCFDCA allows achieving faster settling, less oscillatory stress, and better overall resilience if compared to traditional decentralized or uncoordinated FACTS controllers. The paper also identifies potential benefits of integrating wide-area measurement systems and renewable energy sources, thus opening up the possibilities for scalable and adaptive smart grid applications.

### **REFERENCES:**

- 1. Ibrahim, N. M., El-said, E. A., Attia, H. E., & Hemade, B. A. (2024). Enhancing power system stability: an innovative approach using coordination of FOPID controller for PSS and SVC FACTS device with MFO algorithm. *Electrical Engineering*, 106(3), 2265-2283.
- 2. Barnawi, A. B. (2024). Coordination of Controllers to Development of Wide-Area Control System for Damping Low-Frequency Oscillations Incorporating Large Renewable and Communication Delay. *Arabian Journal for Science and Engineering*, 49(12), 16457-16475.
- 3. He, P., Pan, Z., Fan, J., Tao, Y., & Wang, M. (2024). Coordinated design of PSS and multiple FACTS devices based on the PSO-GA algorithm to improve the stability of wind–PV–thermal-bundled power system. *Electrical Engineering*, 106(2), 2143-2157.
- 4. Arora, A., Bhadu, M., & Kumar, A. (2024). Simultaneous power oscillation damping and frequency control in AC microgrid considering renewable uncertainties: a coordinated control of multiple robust controllers with imperfect communication. *Iranian Journal of Science and Technology, Transactions of Electrical Engineering*, 48(1), 165-185.
- 5. Pandya, M. (2024, August). Rotor Angle Stability Analysis with Coordinated Control of FACTS Devices Using Particle Swarm Optimization. In 2024 IEEE 12th International Conference on Smart Energy Grid Engineering (SEGE) (pp. 42-46). IEEE.
- 6. Bhukya, J., & Singh, P. (2024). Enhancing stability via coordinated control of generators, wind farms, and energy storage: Optimizing system parameters. *Journal of Energy Storage*, 96, 112513.



E-ISSN: 0976-4844 • Website: www.ijaidr.com • Email: editor@ijaidr.com

- 7. Bruno, S., Cometa, R., Ippolito, M. G., La Scala, M., Miglionico, G. C., Musca, R., & Sanseverino, E. R. (2024, July). Power Oscillations Damping Control using BESS with Real-Time PHIL Co-Simulation Validation. In 2024 IEEE Power & Energy Society General Meeting (PESGM) (pp. 1-5). IEEE.
- 8. DONALD, J., NUHU, R., & OGBAKA, D. (2024). MODELLING AND SIMULATION OF POWER SYSTEM PERFORMANCE WITH COORDINATED CONTROL AND INTERACTION OF FACTS CONTROLLERS IN MULTI-MACHINE SURROUNDINGS USING COMBINED UNIFIED POWER FLOW CONTROLLER (C-UPFC). International Journal of Engineering Processing and Safety Research.
- 9. He, P., Yun, L., Fan, J., Wu, X., Pan, Z., & Wang, M. (2024). Coordination of PSS and Multiple FACTS-POD to Improve Stability and Operation Economy of Wind-thermal-bundled Power System. *Recent Advances in Electrical & Electronic Engineering (Formerly Recent Patents on Electrical & Electronic Engineering)*, 17(4), 373-387.
- 10. Sabo, A., Odoh, T. E., Shahinzadeh, H., Wahab, N. I. A., Moazzami, M., & Gharehpetian, G. B. (2024, February). Enhancing power oscillation control: Comparative analysis of damping controllers and hybrid computational intelligence methods for power system stabilization. In 2024 20th CSI International Symposium on Artificial Intelligence and Signal Processing (AISP) (pp. 1-6). IEEE.
- 11. Arora, A., Bhadu, M., & Kumar, A. (2024). Simultaneous damping and frequency control in AC microgrid using coordinated control considering time delay and noise. *Transactions of the Institute of Measurement and Control*, 46(12), 2436-2463.
- 12. Mosleh, M. A. M., & Umurkan, N. (2024). A Novel Techno-Economical Control of UPFC against Cyber-Physical Attacks Considering Power System Interarea Oscillations. *Applied Sciences* (2076-3417), 14(12).
- 13. Nahak, N., & Satapathy, O. (2025). Investigation and damping of electromechanical oscillations for grid integrated micro grid by a novel coordinated governor-fractional power system stabilizer. *Energy Sources, Part A: Recovery, Utilization, and Environmental Effects*, 47(1), 2335-2363.
- 14. Feng, Q., Du, Z., Zhou, D., Yang, X., Pan, A., Zuo, J., & Yang, X. (2025). Research on broadband oscillation characteristics and additional damping control of new energy grid connected systems. *Frontiers in Energy Research*, 13, 1531338.
- 15. Feng, C., Huang, L., He, X., Wang, Y., Dorfler, F., & Kang, C. (2025). Hybrid Oscillation Damping and Inertia Management for Distributed Energy Resources. *IEEE Transactions on Power Systems*.
- 16. Ghatuari, I., & Kumar, N. S. (2025). A Coordinated Control Strategy of Electric Vehicles for Frequency Control in Modern Power Grids. *IEEE Access*.
- 17. Kumar, V., & Koshta, V. Enhanced Small Disturbance Stability of Power Systems through Coordinated Control of D-FACTS.
- 18. Bernal-Sancho, M., Munoz-Lazaro, M., Comech, M. P., & Ferrer-Fernandez, P. (2025). Dynamic Damping of Power Oscillations in High-Renewable-Penetration Grids with FFT-Enabled POD-P Controllers. *Applied Sciences*, 15(3), 1585.
- 19. Mateu-Barriendos, E., Alican, O., Renedo, J., Collados-Rodriguez, C., Martin, M., Nuño, E., ... & Prieto-Araujo, E. (2025). Power oscillation damping controllers for grid-forming power converters in modern power systems. *IEEE Transactions on Power Systems*.
- 20. Satapathy, S., Nahak, N., & Sharma, R. (2025). A Real Time Coordinated Hydro Governor with Dual STATCOM For Low Frequency Oscillation Damping Using Hybrid Mean DE & TVAPSO. *IEEE Access*.



E-ISSN: 0976-4844 • Website: www.ijaidr.com • Email: editor@ijaidr.com

- 21. OYIOGU, D., OBIORA-OKEKE, C. A., & ANIAGBOSO, A. (2024). A Comparative Analysis of STATCOM, SVC, TCSC and UPFC for Voltage Stability and Power loss Reduction in Power System Network. *JAN 2024, IRE Journals*, 7(7).
- 22. Kharayat, P. S., Sharma, S., Gupta, S., & Ahuja, H. (2024, November). Role of FACTS Devices Incorporating Renewable Energy Sources in Distribution and Transmission Systems. In 2024 2nd International Conference on Advancements and Key Challenges in Green Energy and Computing (AKGEC) (pp. 1-6). IEEE.
- 23. Alsulami, S. M., Mobarak, Y. A., & Kannan, N. (2024, September). Enhanced IUPQC Controller for STATCOM based Voltage Regulation for Improved Power Quality in Power System Network. In 2024 International Conference on Communication, Computing and Energy Efficient Technologies (I3CEET) (pp. 96-101). IEEE.
- 24. Kamel, B. K., Attia, M. A., Shaaban, M. F., & Omran, W. A. (2024). Index based techno-economic assessment of FACTS devices installed with wind farms. *IEEE Access*, 12, 19724-19738.
- 25. Fasina, E. T., Adebanji, B., & Oyedokun, J. A. (2024). Power Flow Analysis of the Nigerian Power Grid with FACTS Devices. *Power*, 20(3), 131-136.